ChemPubSoc Europe

DOI: 10.1002/cmdc.201600262

CHEMMEDCHEM Full Papers

Dioxonaphthoimidazoliums are Potent and Selective Rogue Stem Cell Clearing Agents with SOX2-Suppressing Properties

Si-Han Sherman Ho,[a] Azhar Ali,[b] Yi-Cheng Ng,[a] Kuen-Kuen Millie Lam,[c] Shu Wang,[c, d] Woon-Khiong Chan,[c] Tan-Min Chin,[b] and Mei-Lin Go*[a]

Pluripotent stem cells are uniquely positioned for regenerative medicine, but their clinical potential can only be realized if their tumorigenic tendencies are decoupled from their pluripotent properties. Deploying small molecules to remove remnant undifferentiated pluripotent cells, which would otherwise transform into teratomas and teratomacarcinomas, offers several advantages over non-pharmacological methods. Dioxonapthoimidazolium YM155, a survivin suppressant, induced selective and potent cell death of undifferentiated stem cells. Herein, the structural requirements for stemotoxicity were investigated and found to be closely aligned with those essential for cytotoxicity in malignant cells. There was a critical reliance on the quinone and imidazolium moieties but a lesser dependence on ring substituents, which served mainly to fine-tune activity. Several potent analogues were identified which, like YM155, suppressed survivin and decreased SOX2 in stem cells. The decrease in SOX2 would cause an imbalance in pluripotent factors that could potentially prompt cells to differentiate and hence decrease the risk of aberrant teratoma formation. As phosphorylation of the NF-κB p50 subunit was also suppressed, the crosstalk between phospho-p50, SOX2, and survivin could implicate a causal role for NF-κB signaling in mediating the stem cell clearing properties of dioxonaphthoimidazoliums.

Introduction

The clinical potential of stem cell therapy in regenerative medicine is based on two unique characteristics of stem cells: their capacity to proliferate indefinitely while retaining cellular identity (self-renewal) and the ability to differentiate into tissue-specific functional cells when challenged by appropriate differentiation signals (pluripotency).[1] Unfortunately, these traits predispose stem cells toward tumorigenicity, a major hurdle that must be overcome if human pluripotent stem cells (hPSCs) are to be safely deployed for clinical applications.[2,3] The tumorigenic potential of hPSCs is closely linked to the presence of residual pluripotent cells that failed to differentiate.[4] No more than a few thousand cells in differentiated cultures were reportedly sufficient to induce benign teratomas in immunodeficient mice.[5] More menacing is the risk of remnant hPSCs transforming into malignant teratocarcinomas, due to genetic aberrations induced by culture adaptations.[1] To mitigate the problem of aberrant teratogenicity, many conceptually different strategies have been pursued. These include the introduction of suicide genes,[6] genetic selection to remove undesired cell types,[7] extending the time allowed for cells to differentiate,[8] immunodepletion,[9] and the use of cytotoxic antibodies.[10] The deployment of small molecules to selectively remove undifferentiated pluripotent cells has received attention as a viable alternative.[11–13] This pharmacological approach has several advantages: it is robust, rapid, and cost-effective, maintains genetic stability of cells, minimizes cell attrition, and has good translational potential, as it can be applied to complex differentiation protocols. Figure 1 A shows small molecules that have been reported to inhibit the formation of stem-cell-derived teratomas.

The acylphenylhydrazine PluriSin #1 prevented teratoma formation by a mechanism that involved inhibition of stearoyl-CoA desaturase, a key enzyme in the biosynthesis of monosaturated fatty acids.[11] Disruption of this pathway led to ER stress, unfolded protein response, translational attenuation in PSCs, and ultimately, apoptotic cell death. The N-benzylnonanamide JC011, a structural analogue of capsaicin, also induced ER stress by activating the PERK/AT4/DDIT3 pathway.[12] The flavonoid quercetin and dioxonaphthoimidazolium analogue YM155 inhibited survivin, an anti-apoptotic protein whose gene (*BIRC5*) is strongly linked to teratoma formation.[13,14] The rationale for targeting survivin rests on a balance of pro- and anti-apoptotic genes in undifferentiated stem cells.[13] These

[a] *Dr. S.-H. S. Ho, Y.-C. Ng, Prof. M.-L. Go*
Department of Pharmacy, National University of Singapore,
18 Science Drive 4, Singapore 117543 (Singapore)
E-mail: phagoml@nus.edu.sg

[b] *Dr. A. Ali, Dr. T.-M. Chin*
Cancer Science Institute of Singapore,
National University of Singapore,
14 Medical Drive, Singapore 117599 (Singapore)

[c] *Dr. K.-K. M. Lam, Prof. S. Wang, Prof. W.-K. Chan*
Department of Biological Sciences, National University of Singapore,
14 Science Drive 4, Singapore 117543 (Singapore)

[d] *Prof. S. Wang*
Institute of Bioengineering and Nanotechnology,
31 Biopolis Way, Singapore 138669 (Singapore)

Supporting information for this article can be found under http://dx.doi.org/10.1002/cmdc.201600262.

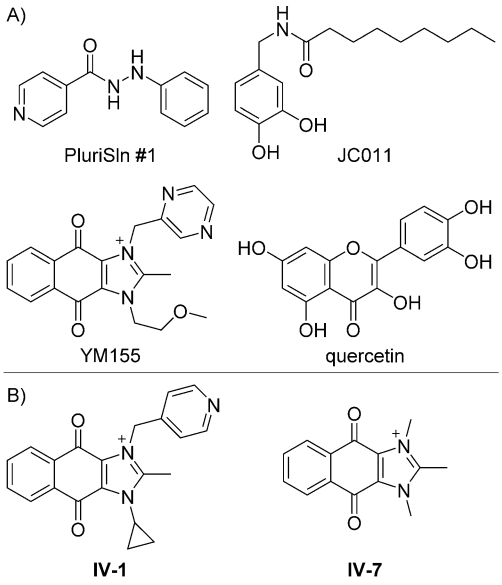

Figure 1. A) Small molecules that have been reported to prevent teratoma formation in stem cell cultures.[11–13] B) Structures of **IV-1** and **IV-7**, which are potent cytotoxic analogues of YM155.[17]

cells express a large number of pro-apoptotic (pro-death) genes and relatively few anti-apoptotic (pro-survival) genes relative to their differentiated counterparts. The survival of stem cells is thus critically dependent on a small number of resident anti-apoptotic genes, and inhibition of these genes or their products would induce apoptosis of undifferentiated stem cells, hence preventing their transition into teratomas. Collateral evidence from YM155 and quercetin confirmed the feasibility of exploiting the differential expression of pro- and anti-apoptotic proteins as a means of suppressing the tumorigenic traits of hPSCs.[13] YM155 (nanomolar IC_{50} value) was significantly more potent than quercetin in this regard by at least 1000-fold.

The outstanding stemotoxic potency of YM155 closely parallels its potent growth inhibitory activity in human malignant cells.[15,16] We previously reported a comprehensive structure–activity relationship (SAR) analysis of the in vitro cytotoxic activity of YM155 and its analogues in non-small-cell lung cancer (NSCLC) cells.[17] Briefly, activity was critically dependent on the quinone moiety and, to a lesser extent, on the positively charged imidazolium ring in the tricyclic naphthoimidazolium scaffold. Substitution on the scaffold served to fine-tune potencies, and our investigations revealed a striking preference for small, compact alkyl substituents on the imidazolium ring. Consequently, we identified two promising analogues—**IV-1** and **IV-7**—which were similar to or exceeded YM155 in terms of growth inhibitory potencies using a panel of NSCLC cells (Figure 1 B). In this context, we asked if these structural requirements were also required for potent stemotoxic activity. From the discovery perspective, a consensus would identify the dioxonaphthoimidazolium ring system as a hit scaffold for stemotoxic activity. Furthermore, with growing evidence that YM155 acts on other bona fide molecular targets besides survivin,[18] overlapping structural requirements allude to the interception of one or more pathways that are common to these different cell types. Scrutiny of these pathways should provide valuable insight into aspects of stem cell biology that are related to cell fate and survival.

Results and Discussion

Growth inhibitory SAR of dioxonaphthoimidazolium analogues in embryonic carcinoma cells

The synthesis and characterization of the library of YM155-related analogues investigated in this report have been described previously.[17] Briefly, the compounds were divided into four series (Series I–IV) based on the structural variations made to the scaffold (Figure 2). Series I compounds were modified at the dioxonaphthoimidazolium core. Series II–IV retained the tricyclic scaffold, and were systematically varied at the substituents attached to N3 (Series II), N1 (Series III), and both N1 and N3 (Series IV).

The compounds were evaluated for growth inhibitory activities in two embryonal carcinoma (EC) cell lines (NCCIT and NTERA-2). EC cells are the malignant counterparts of embryonic stem (ES) cells and are widely employed as models to investigate stem cells, because their growth requirements are less demanding than those of ES cells.[19,20] Tables 1–4 list the growth inhibitory IC_{50} values of the Series I–IV compounds in these cell lines and in non-malignant lung fibroblast IMR-90 cells. IC_{50} values from the two EC cell lines were strongly correlated (Spearman correlation coefficient $\rho = 0.973$, Table S1), implicating a common SAR for both cell lines. We also compared the IC_{50} values from the EC cell lines with those previously reported in malignant NSCLC cells[17] and found, yet again, a sig-

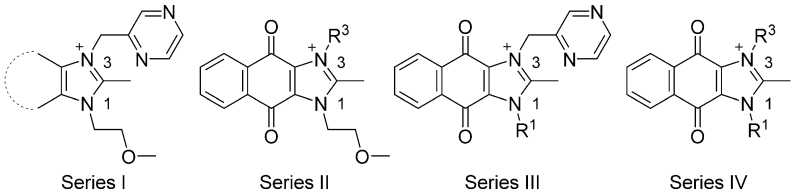

Figure 2. Structural motifs of Series I–IV compounds. Substituents at N1 (R^1) and N3 (R^3) were varied in Series II–IV. In Series I, changes were made to the tricyclic scaffold. In Series II, the N3 side chain of YM155 was modified with no change to the 2′-methoxyethyl side chain at N1. In Series III, the N1 side chain was modified while retaining the N3 2′-pyrazinylmethyl side chain. Series IV combines optimal N1 and N3 groups identified in Series II and III.

Table 1. IC_{50} values of Series I compounds.

Compound		IC_{50} [nM][a] NCCIT	NTERA-2	IMR-90[17]	SI[b]
YM155	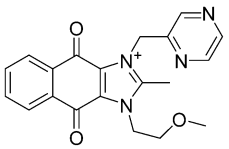	2.09 ± 0.07	1.49 ± 0.08	247 ± 37	142
I-1	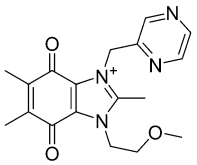	441 ± 32	318 ± 20	1360 ± 150	3.68
I-2	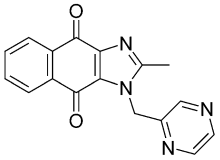	24 000 ± 1000	28 900 ± 3400	55 400 ± 4600	2.11
I-3	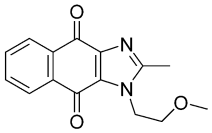	34 300 ± 5700	8290 ± 1190	73 000 ± 4500	5.47
I-4	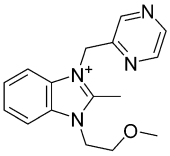	> 100 μM	> 100 μM	> 100 μM	–
I-5	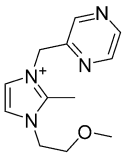	> 100 μM	> 100 μM	> 100 μM	–
I-6	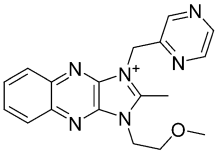	> 100 μM	> 100 μM	> 100 μM	–
I-7	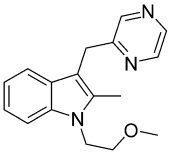	> 100 μM	> 100 μM	> 100 μM	–
I-8	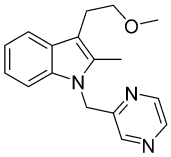	> 100 μM	> 100 μM	> 100 μM	–
I-9	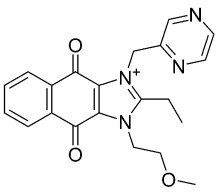	34.8 ± 1.9	19.6 ± 2.0	1900 ± 110	75.8

[a] Evaluated by MTT assay, 72 h incubation, 37 °C, 5% CO_2; values are the mean ± SD of $n = 3$ separate determinations. [b] Selectivity index: (IC_{50} IMR-90)/(mean IC_{50} NCCIT and NTERA-2).

nificant correlation between these activities ($\rho = 0.855–0.920$, Table S1). Thus, we anticipated structural requirements for EC and malignant cells to be broadly similar. However, a comparison of the median IC_{50} values showed that the compounds were at least five- to tenfold more potent in EC cells and had a wider range of potencies (10000-fold in terms of measurable IC_{50} values) as compared to NSCLC cells (1000-fold). In the following paragraphs, SAR is discussed with reference to NCCIT cells and focuses on comparing structural trends deduced from NCCIT and NCSLC cells.

Series I compounds were designed to probe the importance of the intact tricyclic dioxonaphthoimidazolium core. Previously, we showed that any attempt to reduce the tricyclic scaffold to a bicyclic or monocyclic entity invariably led to significant losses in activity, and that of the various motifs in the scaffold, the quinone was the most critical, followed by the positively charged imidazolium, and lastly, the distal benzene ring.[17] These requirements were similarly observed in EC cells. Thus, **I-1**, which lacked the distal phenyl ring but retained the quinone and positively charged imidazolium entities, had nanomolar activity ($IC_{50} = 440$ nM). Analogues with an intact quinone but lacking the positive charge (**I-2** and **I-3**) were strikingly less potent (micromolar IC_{50} values), while the reverse modification (retaining the positive charge without the quinone) gave compounds (**I-4**, **I-5**, and **I-6**) that were conspicuously inactive. Indole analogues **I-7** and **I-8**, which lacked both features, were predictably without activity.

Modifying the substituents on the scaffold, as observed here with the C2-ethyl homologue of YM155 (**I-9**), resulted in only a moderate (tenfold) loss in potency. This was further confirmed in Series II and III, where more extensive side chain variations were made at the imidazolium nitrogen atoms (Tables 2 and 3). IC_{50} values ranged from 2 to 2400 nM for Series II (median 24 nM) and from 5 to 1400 nM (median 37 nM) for Series III. Tellingly, even the weakest analogues in both series retained single digit micromolar growth inhibitory activities, underscoring a largely differentiating role for substituents on the scaffold.

Analysis of the Series II compounds revealed several structural requirements that were common for NSCLC cells. We noted a preference for azinylmethyl side chains at N3. Analogues with non-azinylmethyl residues (benzyl **II-1**, cyclohexylmethyl **II-2**, thienylmethyl **II-3**, and imidazolylmethyl **II-4**) were less active. Non-ring-bearing side chains (**II-15** to **II-22**) were also not favored. We further noted a regioisomeric bias against azines with *ortho*-azomethine nitrogen atoms (**II-5** and **II-8** versus **II-6**, **II-7**, and **II-9**–**II-11**). Interestingly, the adverse effect of an *ortho*-nitrogen could be overruled by the concurrent presence of a *para*-nitrogen (**II-9**) or a *meta*-nitrogen (YM155). The importance of the *para*-nitrogen was further highlighted in **II-12**, where a methyl substituent at the *para* position of the pyrazinylmethyl ring elicited a steep loss in activity. Additionally, we noted the importance of maintaining a methylene linker between N3 and pyrazine, as seen from the diminished activities of homologues **II-13** and **II-14**.

Differences in structural requirements were also recognized, but these were mainly quantitative. Notably, the N3-alkyl-bearing analogues (**II-15** to **II-21**) had IC_{50} values that fell within a narrow threefold range (26–60 nM), in contrast to the wider tenfold variation (29–280 nM) for the same compounds in NSCLC cells.[17] The tighter activity range meant that it was harder to identify an optimal alkyl substituent. The N3-methyl analogue **II-15** is illustrative. Compound **II-15** was the most potent Series II analogue in NSCLC cells, but in NCCIT cells, it was no better than the ethyl (**II-16**), *n*-propyl (**II-17**) or cyclopropyl (**II-19**) homologues.

Several SAR similarities were also detected in Series III. These were losses in activity when the 2′-methoxyethyl side chain at N1 was modified by demethylation (**III-1**), homologation (**III-2**), or functionalization with substituted amino groups (**III-3** and **III-4**). There was also a limited tolerance for ring-bearing substituents at N1, as seen from the tetrahydrofuranylmethyl (**III-5**), benzyl (**III-6**), and pyrazinylmethyl (**III-7**) compounds, and a preference for N1-alkyl substituents that were unbranched (**III-10** versus **III-14**; **III-11** versus **III-15**) and sterically compact (cyclopropyl **III-12** versus cyclopentyl **III-13**). In a departure from Series II, homologation from a methyl (**III-8**) to an *n*-butyl (**III-11**) moiety in Series III identified the *n*-propyl to be optimal. Cyclization of *n*-propyl (**III-10**) to a cyclopropyl (**III-12**) did not yield a clear advantage. No outstanding differences were observed between the SAR trends for EC and NSCLC cells for this series.

Series IV incorporated highly ranked substituents identified from Series II (pyridin-3- or 4-ylmethyl, pyridimin-5-ylmethyl at N3) and Series III (ethyl or cyclopropyl at N1), based on growth potencies determined in NSCLC cells.[17] These substituents were also optimal in EC cells and were thus investigated to determine if their concurrent presence on the same molecule would result in superior activity. Disappointingly, this was not the case, and only one analogue (**IV-1**, $IC_{50} = 2.6$ nM) narrowly approached the activity of YM155 ($IC_{50} = 2.1$ nM). The N^1,N^3-dimethyl analogue **IV-7** should be mentioned, because it was the most potent analogue in NSCLC cells ($IC_{50} = 8–18$ nM versus 14–36 nM for YM155)[17] but had mediocre activity in EC cells ($IC_{50} = 6.1–24$ nM versus 1.5–2.1 nM for YM155).

In summary, we found a striking overlap in the structural requirements for potent growth inhibitory activities in dioxonaphthoimidazolium analogues in both EC and NSCLC cell lines. In both instances, reducing the tricyclic scaffold to a bicyclic or monocyclic entity resulted in significant losses in activity. Thus, the intact dioxonaphthoimidazolium scaffold was obligatory for potent activity. Of the various motifs in the scaffold, the quinone was the most critical, followed by the charged imidazolium ring, and lastly, the distal benzene ring. Functionalization at N1 and N3 served mainly to fine-tune activity, and potency differences in the resulting compounds were narrow and still within the nanomolar range. Azinylmethyl side chains were preferred at N3, whereas unbranched non-cyclized alkyl groups were favored at N1. Several compounds (**II-7**, **II-9**, **III-12**, and **IV-1**) were comparable to YM155 in terms of activity but none exceeded it by twofold or more.

Table 2. IC_{50} values of Series II compounds.

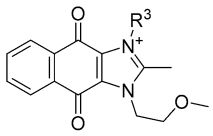

Compd	R^3	IC_{50} [nM][a] NCCIT	NTERA-2	IMR-90[17]	SI[b]
II-1	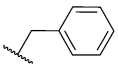	43.7 ± 3.2	31.9 ± 3.9	1160 ± 70	31.4
II-2	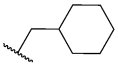	75.6 ± 11.8	30.8 ± 3.4	5270 ± 960	120
II-3	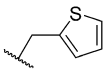	53.6 ± 1.5	44.2 ± 7.3	1450 ± 50	29.9
II-4	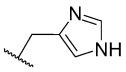	76.6 ± 8.6	71.6 ± 1.5	2010 ± 110	27.2
II-5	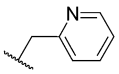	19.7 ± 3.3	13.8 ± 1.0	2520 ± 110	155
II-6	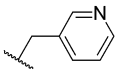	5.46 ± 0.32	3.79 ± 0.55	611 ± 44	137
II-7	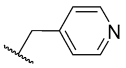	1.99 ± 0.26	1.55 ± 0.15	176 ± 9	101
II-8	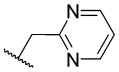	25.7 ± 4.7	9.36 ± 1.83	3180 ± 40	232
II-9	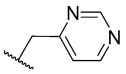	2.23 ± 0.11	1.98 ± 0.40	205 ± 14	97.7
II-10	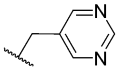	6.22 ± 0.58	4.62 ± 0.22	276 ± 27	52.1
II-11	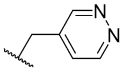	5.51 ± 0.99	3.63 ± 0.43	187 ± 12	42.7
II-12	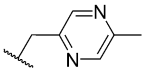	20.6 ± 1.98	10.6 ± 0.8	2000 ± 130	143
II-13	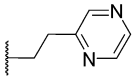	104 ± 8	52.0 ± 2.4	2810 ± 520	40.5
II-14		2411 ± 175	2803 ± 506	8820 ± 1210	3.40
II-15		26.2 ± 0.9	12.3 ± 1.6	345 ± 38	20.6
II-16		22.2 ± 2.2	12.9 ± 1.5	1230 ± 130	75.4
II-17		24.2 ± 3.5	16.4 ± 3	1720 ± 83	88.0
II-18	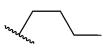	45.1 ± 4.0	17.3 ± 1.0	2640 ± 540	106
II-19		24.0 ± 0.6	12.0 ± 2.3	1160 ± 140	72.5
II-20		60.3 ± 2.8	35.3 ± 5.9	3890 ± 290	87.3
II-21		57.1 ± 7.0	23.2 ± 3.7	6790 ± 290	206

These are not the final page numbers! ↗↗

Table 2. (Continued)

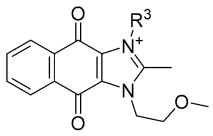

Compd	R^3	IC_{50} [nM][a] NCCIT	NTERA-2	IMR-90[17]	SI[b]
II-22	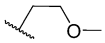	17.8 ± 1.94	13.2 ± 0.9	743 ± 89	49.0

[a] Evaluated by MTT assay, 72 h incubation, 37 °C, 5% CO_2; values are the mean ± SD of $n = 3$ separate determinations. The range of measurable values was 1.99 nM–2.4 μM for NCCIT (median 25 nM) and 1.55 nM–2.8 μM for NTERA-2 (median 13.5 nM). [b] Selectivity index: (IC_{50} IMR-90)/(mean IC_{50} NCCIT and NTERA-2).

Table 3. IC_{50} values of Series III compounds.

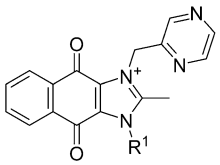

Compd	R^1	IC_{50} [nM][a] NCCIT	NTERA-2	IMR-90[17]	SI[b]
III-1	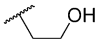	25.6 ± 2.8	21.1 ± 3.3	2480 ± 320	107
III-2	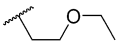	21.9 ± 1.04	13.8 ± 0.7	1430 ± 260	84.5
III-3	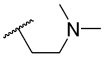	501 ± 90	512 ± 30	7420 ± 760	14.6
III-4	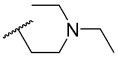	1364 ± 71	919 ± 74	3730 ± 110	3.40
III-5	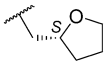	188 ± 9	56.4 ± 9.6	9890 ± 170	114
III-6	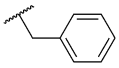	149 ± 5	105 ± 14	5610 ± 380	45.5
III-7	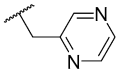	59.1 ± 5.7	19.0 ± 1.8	3570 ± 710	124
III-8		13.8 ± 1.8	7.62 ± 1.37	582 ± 89	59
III-9		8.86 ± 0.85	3.63 ± 0.56	480 ± 22	93.2
III-10		5.71 ± 0.82	3.45 ± 0.67	565 ± 27	131
III-11	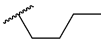	10.2 ± 1.1	4.69 ± 0.26	1620 ± 140	252
III-12		4.88 ± 0.57	1.99 ± 0.30	213 ± 20	75.3
III-13		158 ± 3	109 ± 23	6580 ± 180	50.6
III-14		20.9 ± 2.1	13.5 ± 2.8	1420 ± 150	86.7
III-15		48.4 ± 1.4	31.4 ± 2.9	7970 ± 180	209

[a] Evaluated by MTT assay, 72 h incubation, 37 °C, 5% CO_2; values are the mean ± SD of $n = 3$ separate determinations. Range of measurable values was 4.88 nM–1.36 μM for NCCIT (median 25.6 nM) and 1.99 nM–919 nM for NTERA-2 (median 19.0 nM). [b] Selectivity index: (IC_{50} IMR-90)/(mean IC_{50} NCCIT and NTERA-2).

Table 4. IC_{50} values of Series IV compounds.

Compound		IC_{50} [nM][a] NCCIT	NTERA-2	IMR-90[17]	SI[b]
IV-1	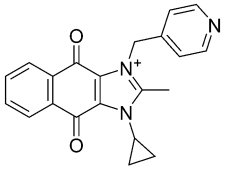	2.46 ± 0.20	2.56 ± 0.25	287 ± 59	115
IV-2	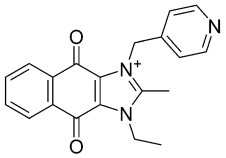	7.61 ± 1.03	4.44 ± 0.35	310 ± 51	55.3
IV-3	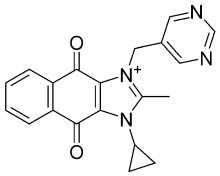	40.5 ± 2.4	34.6 ± 0.8	649 ± 79	17.4
IV-4	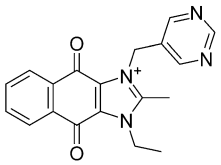	20.1 ± 2.1	15.2 ± 0.9	440 ± 7	25.4
IV-5	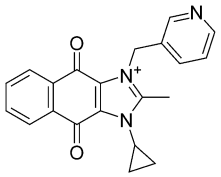	10.4 ± 1.4	9.15 ± 0.92	484 ± 64	49.7
IV-6	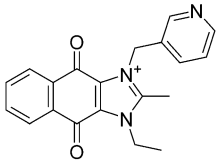	8.38 ± 0.54	5.72 ± 0.48	475 ± 91	69.9
IV-7	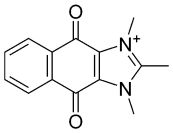	24.2 ± 2.0	6.08 ± 0.60	159 ± 16	16.4
YM155	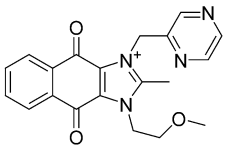	2.09 ± 0.07	1.49 ± 0.08	247 ± 37	142

[a] Evaluated by MTT assay, 72 h incubation, 37 °C, 5% CO_2; values are the mean ± SD of $n = 3$ separate determinations. [b] Selectivity index: (IC_{50} IMR-90)/(mean IC_{50} NCCIT and NTERA-2).

Selective cytotoxicity for embryonic carcinoma cells

Tables 1–4 also list the selectivity ratios of Series I–IV compounds, based on a comparison of IC_{50} values derived from human lung fibroblast IMR-90 cells and the mean IC_{50} values from NCCIT and NTERA cells. YM155 and its analogues were selectively more cytotoxic toward EC cells, with ratios ranging from 2 (**I-2**) to 250 (**III-11**). Tellingly, they were significantly more selective against EC cells than NSCLC cells, in which no more than a 20-fold variation (2 to 38) was observed.[17] We were further encouraged to find that potent analogues like **II-7**, **II-9**, **III-12**, and **IV-1** were at least 70-fold more cytotoxic toward EC cells. More intriguing were the outstanding selectiv-

ities (≥200) of **II-8**, **II-21**, **III-11**, and **III-15** (IC_{50} values of 5–57 nM), which were admittedly less potent than YM155 but promising stemotoxic candidates in view of their exceptionally selective cytotoxicities.

Growth inhibitory activity of YM155 and selected analogues toward other stem cell lines

We next proceeded to determine if the potent growth inhibitory activities of the YM155 analogues would be replicated in other stem cell types. Hence, YM155 and seven analogues (**II-7**, **II-13**, **III-6**, **III-13**, **IV-1**, **IV-2**, and **IV-7**) were evaluated in a human ES cell line (H9) and an induced pluripotent stem (iPS) cell line (HCT-8 3.11). HCT-8 3.11 was derived from its non-stem-cell progenitor HCT-8, a colorectal carcinoma cell line, by transfection of the Yamanaka factors (SOX2, OCT4, KLF4, and c-MYC).[21,22] Results are given in Table 5.

Table 5. IC_{50} values of YM155 and analogues on embryonic stem cell line H9, induced pluripotent stem cell line HCT-8 3.11, and non-stem cell progenitor HCT-8 cells.

Compd	IC_{50} [nM][a]			
	H9[b]	HCT-8 3.11[c]	HCT-8[c]	NTERA-2/NCCIT[d]
YM155	10.0±1.6	6.43±0.97	21.8±2.6	1.5/2.1
II-7	11.6±1.6	7.26±1.32	11.8±0.5	1.6/2.0
II-13	174±7	215±41	1210±152	52/104
III-6	739±148	604±80	2130±367	110/150
III-13	156±31	367±71	1250±269	110/160
IV-1	4.21±0.49	5.47±0.80	15.4±2.3	2.5/2.6
IV-2	4.31±0.54	7.66±1.00	28.9±1.7	4.4/7.6
IV-7	24.9±0.2	13.9±1.5	32.9±1.5	6.1/24

[a] Values are the mean±SD of $n=3$ separate determinations. [b] Determined by MTT assay after 24 h incubation. [c] Determined by MTT assay after 72 h incubation. [d] IC_{50} values of EC cells were included for comparison.

The analogues were selected to cover a range of potencies, as determined by IC_{50} values in EC cells: **II-7** and **IV-1** (potent, $IC_{50}=2$–3 nM, comparable to YM155); **IV-2** and **IV-7** (moderately potent, $IC_{50}=5$-25 nM); and **II-13**, **III-6**, and **III-13** (weakly potent, $IC_{50}=50$–160 nM).[17] The results showed that the test compounds, including YM155, were generally less potent toward ES (H9) and iPS (HCT-8 3.11) cells. Changes in the rank order of potencies were also detected and were most evident among the more potent compounds. Thus, only **IV-1** and not **II-7** was highly ranked against H9 and HCT-8 3.11. No change was found in the rank order of the weakly potent analogues which remained poorly active in both H9 and HCT-8 3.11 cells. The analogues displayed differential growth activities toward HCT-8 and HCT-8 3.11, with greater potencies (1.5- to fivefold higher) in the iPS cell line.

Figure 3 shows the effects of **IV-1** and YM155 on the morphology of a co-culture of H9 and mouse embryonic fibroblasts (MEF), which were feeder cells for H9. In untreated cells, the spindle-shaped MEF cells were readily distinguished from the colony-forming H9 cells. When treated with YM155 or **IV-1**,

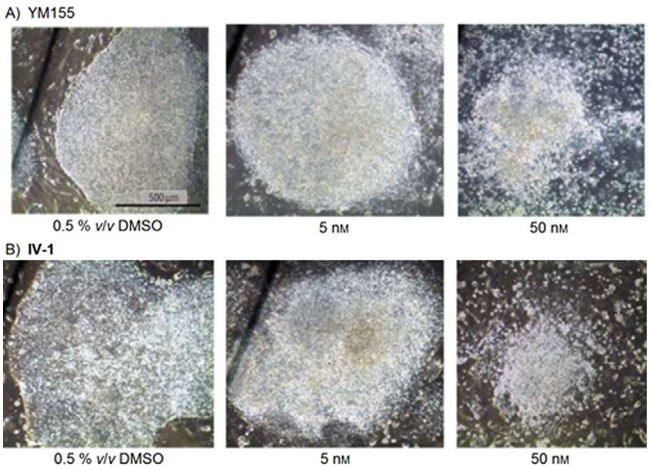

Figure 3. Morphology of H9–MEF co-cultures following 24 h treatment with 5 and 50 nM A) YM155 and B) **IV-1**. Control co-cultures were treated with 0.5% DMSO in media. The characteristic clear demarcation of H9 colonies were lost at 50 nM YM155 and **IV-1**. Images presented are representative of triplicate experiments performed under each treatment condition. Scale bar (500 µm) for YM155 control applies to other figures.

the boundaries demarcating the H9 colonies became progressively blurred, indicating that the H9 cells had lost their viabilities. This was particularly marked in cells treated with 50 nM YM155 or **IV-1**. In contrast, the MEF cells retained their morphology and remained viable under these conditions. Thus, the cytotoxicities of **IV-1** and YM155 were selectively directed against H9 cells, as was observed earlier in EC cells.

YM155, IV-1, and IV-7 decrease SOX2 expression in an EC cell line

To inhibit the formation of stem cell-derived teratomas, an agent should potently and selectively eliminate residual stem cells that are intermixed with terminally differentiated cell populations designated for clinical use. If the remnant cells could also be induced to differentiate, this would further repress their tumorigenic potential.[1] Pluripotency is regulated by transcription factors such as OCT4, SOX2, MYC, KLF4, NANOG, and LIN28, combinations of which have been successfully used to induce the reversion of somatic cells to a stem-cell-like state.[21–23] Many of these transcription factors are oncogenes or are highly expressed in various types of cancer. Many oncogenic signaling pathways are intercepted by YM155.[24,25] Thus, we asked if YM155 and its analogues could augment their cytotoxicity toward stem cells by suppressing pluripotent markers, promoting cell differentiation, and thus efficiently obviating teratoma formation. Hence, we examined the effects of YM155 and its potent analogue, **IV-1**, on OCT4, SOX2, and NANOG, which are core components of the regulatory network responsible for maintaining the pluripotent state of stem cells.[26,27]

First, we probed the mRNA expression of these transcription factors using qRT-PCR in NCCIT, H9, and HCT-8 3.11 cells treated with YM155, **IV-1**, and **IV-7** at their IC_{50} concentrations. The analysis was carried out at 12 h and 24 h for NCCIT and H9

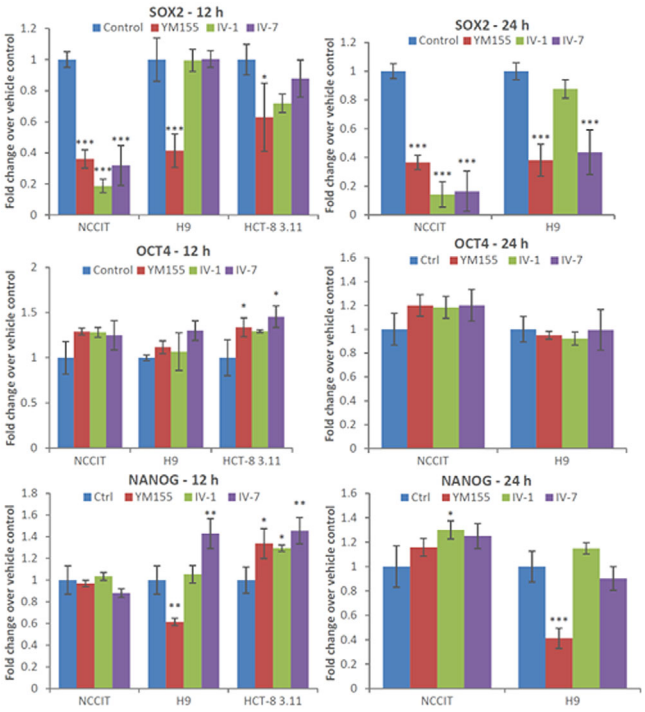

Figure 4. Expression of SOX2, OCT4, and NANOG mRNAs following 12 or 24 h of treatment with YM155, **IV-1**, or **IV-7**, quantified by qRT-PCR. IC_{50} values at 24 h were found to be: YM155: 10 nM (NCCIT and H9) and 15 nM (HCT-8 3.11); **IV-1**: 30 nM (NCCIT), 4 nM (H9), and 20 nM (HCT-8 3.11); and **IV-7**: 150 nM (NCCIT), 25 nM (H9), and 40 nM (HCT-8 3.11). mRNA levels of the housekeeping gene GAPDH were used for normalization. Bars represent the fold change of cDNA normalized against GAPDH in the same sample. Error bars represent the SD of three separate experiments. Significant statistical difference from vehicle control: $*p<0.05$, $**p<0.01$, $***p<0.001$ (Tukey post-hoc test of respective populations of treated groups vs. control).

cells but limited to 12 h for the iPS cell line. As shorter treatment times were deployed, the IC_{50} values of these compounds were re-determined at 24 h to ensure that pharmacologically relevant concentrations were used.

Figure 4 shows the fold change in mRNA expression of SOX2, OCT4, and NANOG in treated cells after incubation. Variable trends were observed depending on cell type and test compound. On the basis of cell type, we noted that SOX2 mRNA levels in treated NCCIT cells were significantly reduced at both time points. In contrast, OCT4 and NANOG levels were unchanged. In H9 cells, only YM155 significantly reduced the transcription of SOX2 and NANOG within 12 h. The transcription of SOX2 in H9 was also reduced by **IV-7**, but only after 24 h. None of the transcription factors in H9 were perturbed by **IV-1**. In HCT-8 3.11, we found that only YM155-treated cells showed a decrease in SOX2 mRNA. Thus, YM155 consistently reduced SOX2 levels in all cell lines (NCCIT, H9, and HCT8 3.11). In HCT-8 3.11 cells, we noted increases in OCT4 and NANOG, a trend that was not found with the other stem cell lines. As a significant proportion of OCT4 and NANOG expression in HCT-8 3.11 was due to transfected genes, we speculated that these genes may not be regulated in the same way as the native gene, which could have given rise to the observed increases.

Taken together, we deduced that SOX2 was most susceptible to perturbation. It was reduced by all three test compounds in treated NCCIT cells, by YM155 and **IV-7** in H9 cells, and by YM155 only in HCT-8 3.11 cells. In contrast, OCT4 levels were unchanged in NCCIT and H9 cells but increased in HCT8 3.11. The susceptibility of NANOG to perturbation was intermediate, as it was observed in two cell lines, namely H9 (YM155 caused a reduction) and HCT-8 3.11 (all test compounds resulted in increases).

As the transcription of SOX2 mRNA was diminished in most of the treated cell lines, we proceeded to determine if SOX2 protein levels would be similarly affected. To this end, we treated NCCIT and HCT-8 3.11 cells with YM155 and **IV-1** at their IC_{50} and $2\times IC_{50}$ concentrations for 48 h and probed for SOX2 by immunoblotting. As shown in Figure 5, SOX2 levels were

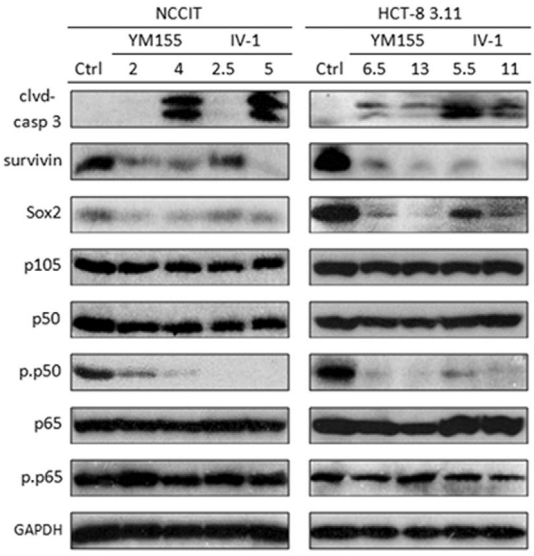

Figure 5. Levels of cleaved caspase 3, survivin, SOX2, and NF-κB subunits p50, p65, and p105 and their phosphorylated forms (p.p50, p.p65) in NCCIT and HCT-8 3.11 cells after treatment with YM155 and **IV-1** for 48 h. GAPDH was used as a loading control. YM155 and **IV-1** were tested at their IC_{50} and $2\times IC_{50}$ concentrations. IC_{50} values of YM155 and **IV-1** in NCCIT and HCT-8 3.11 cells are mentioned in Table 5.

indeed reduced by YM155 and **IV-1** in both cell lines. We also monitored the levels of the apoptotic marker proteins survivin and cleaved caspase 3. The losses in survivin and appearance of cleaved caspase 3 recapitulate the induction of apoptosis by YM155 and **IV-1**.

The pluripotent state of human embryonic stem cells is maintained by a network of transcription factors, of which SOX2, OCT4, and NANOG have been widely identified as core components.[28,29] The prevailing model advocates cooperativity between the pluripotency factors as central to self-renewal and pluripotency,[27] while a contrarian view proposes a modular pluripotency network in hESCs in which each transcription factor controls specific cell fates, and there is limited overlap in the regulation of their gene expression.[30] Clearly, there are gaps in our understanding of the molecular mechanisms and interactions underlying the roles of these factors in pluripoten-

cy. Our results showed that SOX2 was selectively targeted by YM155 and its potent analogues in different stem cell types, with significant decreases elicited at both transcriptional and protein levels. In our view, the ensuing imbalance in pluripotency factors (unchanged OCT4 and NANOG, decrease in SOX2) would invariably affect the ability of the cells to remain in their pluripotent states.

YM155 and IV-1 suppress activation of NF-κB subunit p50 in NCCIT and HCT-8 3.11 cells

We have previously shown that YM155 and **IV-1** intercepted the phosphorylation of the NF-κB subunit p50, which regulates the binding of NF-κB dimers to DNA and transcription of NF-κB-controlled genes in NSCLC cell lines.[31] p50 forms a heterodimer with p65, another NF-κB subunit, which then binds to DNA sequences on NF-κB response elements to trigger transcription of NF-κB-controlled genes. The phosphorylation of p50 controls the binding process, whereas phosphorylation of p65 affects transcription. Interception of either process inhibits the signaling pathway. We proposed that the pleiotropy that is increasingly cited for YM155 may be attributed in part to the intervention of this pathway. NF-κB signaling has wide-ranging effects on the expression of apoptotic proteins like survivin, Mcl-1, and Bcl-xl, which are downregulated by YM155 and its analogues.[31]

The role of NF-κB signaling in maintaining pluripotency of iPSCs was highlighted by Takase et al.,[32] who showed that the pathway was upregulated in undifferentiated iPSCs. When suppressed by p65 siRNA, expression of OCT4 and NANOG was reduced. Furthermore, disrupting the NF-κB pathway in hESCs led to the downregulation of SOX2, OCT4, and NANOG.[33] Within this context, we were curious if our earlier observations on the interception of p50 phosphorylation by YM155 and **IV-1** in malignant cells extended to hESCs as well. Thus, we probed the levels of p65, p50, p105 (a precursor of p50), phospho-p65, and phospho-p50 in NCCIT and HCT8 3.11 cells treated with YM155 and **IV-1** under conditions described in the preceding section (Figure 5). Our results showed no change in p65 and its activated state (phospho-p65) in the treated cells. Levels of p50 and p105, the inactive precursor of p50, were similarly unaltered. On the other hand, phospho-p50 was significantly reduced by both compounds, which coincided with our earlier findings in malignant cells.

Conclusions

Our investigations provided insight into the potential of YM155 and its analogues as agents for the eradication of remnant stem cells from differentiated cell populations. The efficient and selective induction of cell death of human pluripotent stem cells, first observed with YM155, was shown here to be closely associated with other dioxonaphthoimidazolium analogues. A definitive SAR that closely parallels that established for normal malignant cells was evident. YM155 and its potent analogue, **IV-1**, induced an imbalance in pluripotent factors by downregulating SOX2 at gene and protein levels. Such an action would influence cell fate and, if cells are thus prompted to differentiate, the risk of remnant undifferentiated cells transforming into the malignant phenotype would be lowered. Dioxonaphthoimidazoliums would then have a dual approach in overcoming the tumorigenicity hurdle: inducing apoptosis and promoting terminal differentiation of residual stem cells.

The overlapping structural requirements for stemotoxic and cytotoxic activities implicate the involvement of similar mechanisms in the induction of cell death by the dioxonaphthoimidazolium analogues. In this regard, the interception of NF-κB by YM155 and **IV-1** in both stem cells and malignant cells was interesting. NF-κB signaling is augmented in stem cells and is important for maintaining their self-renewal and pluripotency. Disruption of this pathway was reported to significantly decrease SOX2, NANOG, and OCT4 in ES and iPS cells.[32,33] Survivin overexpression is the biological sequela of NF-κB activation in several malignancies.[34] Taken together, the ability of YM155 and **IV-1** to concurrently suppress survivin, phospho-p50, and SOX2 in stem cells (NCCIT, HCT-8 3.11) implicate a causal role for the NF-κB pathway. Inhibition of p50 phosphorylation would disrupt gene transcription, and if the affected gene products are involved in cell differentiation and survival (like SOX2 and survivin), teratoma formation would be effectively curtailed.

Experimental Section

Synthesis and characterization of Series I–IV compounds: Synthesis and characterization of compounds in Series I–IV were described previously.[17] Compounds were characterized by ^{1}H NMR and ^{13}C NMR spectroscopy, nominal or high-resolution masses were determined by LC–MS, and purity was assessed by reverse-phase HPLC on two solvent systems and found to be $\geq$95%. A brief overview of the synthetic schemes for Series II, III, and IV and spectroscopic data for potent analogues **IV-1** and **IV-7** are presented in the Supporting Information.

Cell culture conditions for NCCIT, NTERA-2, HCT-8, and HCT-8 3.11: Human pluripotent EC cell lines (NCCIT and NTERA-2) and human colorectal carcinoma cells line HCT-8 were obtained from American Type Culture Collection (ATCC, Manassas, VA, USA). HCT-8 3.11, an induced pluripotent stem cell line, was generated from HCT-8 using a baculovirus vector to transfect Yamanaka factors into the parental line. RPMI-1640 and DMEM were supplemented with 10% heat-inactivated fetal bovine serum (FBS) and 0.01% *w/v* penicillin G–streptomycin before culturing. NCCIT cells were maintained in RPMI-1640, while NTERA-2 and HCT-8 cells were maintained in DMEM. The DMEM/F-12 (1:1) media (Hyclone, GE Healthcare, Buckinghamshire, UK) was supplemented with 1% FBS, 0.005% penicillin G–streptomycin, 5 mL GlutaMax (Gibco, Life Technologies Corporation, Carlsbad, CA, USA), and epidermal growth factor (Peprotech, Rocky Hill, NJ, USA) for the growth of HCT-8 3.11 cells. Cells were passaged upon reaching 80% confluence.

Cell culture conditions for H9: The H9 and MEF cell lines originated from WiCell Research Institute (Madison, WI, USA). H9 cells were maintained in DMEM/F-12 (1:1) (Gibco), prepared according to the formulation described in the Supporting Information (Table S2). MEF cells were maintained in high glucose DMEM (Gibco), supplemented with 10% FBS, 2 mM L-glutamine, and 0.1 mM nonessential amino acids solution. Culture dishes (35 mm) were coated with

0.1% gelatin (1 mL) and incubated at 37 °C for 1 h. Gamma-irradiated MEF cells were seeded in each gelatin-coated dish (3×10^5 cells per dish) and incubated for 24 h for adhesion to the dish. Post-adhesion, the MEF layer was washed once with phosphate-buffered saline (PBS) and ~100–120 H9 colonies, suspended in H9 media, were seeded. Media was changed daily, and passaging was performed every 5–7 days, depending on the size of the colonies. During passaging, each large colony was carefully separated into 200–300 μm pieces using a small scalpel. Roughly 100–120 pieces were then collected and seeded on another culture dish previously seeded with MEF cells.

Growth inhibitory MTT assay: MEFs were seeded in each well of a 24-well plate (5×10^4 cells per well) and left overnight for attachment. H9 cells were then seeded at a density of 8×10^4 cells per well. The co-culture was incubated for 48 h, with media changed every 24 h, before treatment with test compounds. Other cell lines were seeded in 96-well plates at the following densities and incubated for 24 h before treatment: 3×10^3 (HCT-8 and HCT-8 3.11), 4×10^3 (NTERA-2, IMR-90) and 6×10^3 (NCCIT) cells per well. Thereafter, media in each well was aspirated and replaced with 497.5 μL (H9) or 199 μL (other cell lines) of media and 2.5 μL (H9) or 1 μL (other cell lines) of test compound (prepared in DMSO stock solution at a 200-fold higher concentration). After 24 h (H9) or 72 h (other cell lines), media was aspirated before adding an aliquot of 0.5 mg mL^{-1} MTT (Alfa Aesar, Lancashire, UK) in media and incubating for 2–3 h. The resulting formazan crystals were dissolved in DMSO and quantified at 570 nm on a microplate reader (Tecan Infinite M2000 Pro, Männedorf, Switzerland). Viable cells were determined from the following equation for HCT-8, HCT-8 3.11, NCCIT, and NTERA-2 [Eq. (1)]:

$$\text{Percentage viability} = \frac{A_{\text{compound}} - A_{\text{blank}}}{A_{\text{control}} - A_{\text{blank}}} \times 100\,\% \quad (1)$$

for which A_{compound} is the average absorbance of compound-treated cells, A_{control} is the average absorbance of untreated (control) cells, and A_{blank} is the average of absorbance of DMSO.

For H9, a set of background controls were prepared by seeding only MEF cells in the well. Each H9–MEF well was compared with a MEF control well (both subjected to the same treatment conditions) to isolate the response of H9 to treatment using Equation (2):

$$\text{Percentage viability} = \frac{A_{\text{t}} - A_{\text{blank,t}}}{A_{\text{control}} - A_{\text{blank, control}}} \times 100\,\% \quad (2)$$

for which A_{t} is the average absorbance of compound-treated H9–MEF wells, $A_{\text{blank,t}}$ is the average absorbance of compound-treated MEF-only wells, A_{control} is the average absorbance of untreated (control) H9–MEF wells, and $A_{\text{blank,control}}$ is the average absorbance of untreated (control) MEF-only wells.

The IC_{50} value (the concentration of test compound required to inhibit cell growth by 50%) was determined by plotting the percentage viability against the logarithmic concentration of test compound using GraphPad Prism 6 (GraphPad Software, Inc., USA).

qRT-PCR: NCCIT, H9, and HCT-8 3.11 cells were seeded at 8.0×10^5 cells per well in six-well plates for 24 h followed by exposure to test compound for 12 h or 24 h. RNA extraction was performed following the manufacturer's protocol (RNeasy Mini Kit, Qiagen, Venlo, Netherlands). RNA content was quantified using a ND-1000 spectrophotometer (NanoDrop Technologies, Wilmington, DE, USA). All samples showed OD_{260}/OD_{280} ratios between 1.73 and 2.11, with concentrations ranging from ~400 to ~1200 ng μL^{-1}. Results from an Agilent Bioanalyzer 2000 analysis (Agilent Technologies, Santa Clara, CA, USA) showed that all samples had RNA integrity numbers (RINs) of 9.4–10. RNA (1.7 μg) was withdrawn from each sample for cDNA synthesis using Promega M-MLV reverse transcriptase following the recommended protocol (Promega Life Sciences, Madison, WI, USA). Five primers, corresponding to SOX2, NANOG, OCT4, and GAPDH, were obtained from AIT Biotech (Singapore) based on sequences sourced from PrimerBank (Harvard Medical School, Boston, MA, USA). PCR was carried out in a volume of 20 μL using SYBR Green dye on an Applied Biosystem 7500 Fast Real Time PCR system (Thermo Fisher Scientific, Waltham, MA, USA). Data analysis was performed using a comparative C_T (threshold cycle) method and normalized to GAPDH expression levels.

Western blotting: Cells were seeded at the following densities (per dish) in 100 mm petri dishes and incubated for 24 h for attachment: NCCIT = 6×10^5 cells, HCT-8 3.11 = 1.2×10^6 cells. Media was aspirated and replaced by 10 mL fresh media containing test compound. After 48 h incubation, cells were harvested and lysed in Cellytic M buffer (Sigma–Aldrich, St. Louis, MO, USA). Protein content was assessed by Bradford assay (Bio-Rad, Hercules, CA, USA) and subjected to SDS-PAGE after standardization of protein content. Proteins were blocked in 5% nonfat milk and probed with antibodies against cleaved caspase 3, survivin, native and phosphorylated forms of p50/p105, p65 (Cell Signaling Technology, Danvers, MA, USA), and SOX2 (Santa Cruz Biotech, Santa Cruz, CA, USA). Anti-GADPH antibody (Santa Cruz Biotech) was used as a loading control. WesternBright ECL or Quantum (Advansta, Menlo Park, CA, USA) were added following incubation with horseradish peroxidase-conjugated anti-mouse, anti-rabbit, and anti-goat secondary antibodies (Santa Cruz Biotech) to visualize bands.

Acknowledgements

This work was supported by a Ministry of Education Faculty Research Grant (R148000188112) to M.L.G. S.H. gratefully acknowledges scholarship support from the Ministry of Education, Singapore.

Keywords: antiproliferation · dioxonaphthoimidazoliums · factor SOX2 · stem cell clearing agents · structure–activity relationships

[1] U. Ben-David, N. Benvenisty, *Nat. Rev. Cancer* **2011**, *11*, 268–277.
[2] P. S. Knoepfler, *Stem Cells* **2009**, *27*, 1050–1056.
[3] J. M. Brickman, T. G. Burdon, *Nat. Genet.* **2002**, *32*, 557–558.
[4] K. Miura, Y. Okada, T. Aoi, A. Okada, K. Takahashi, K. Okita, M. Nakagawa, M. Koyanagi, K. Tanabe, M. Ohnuki, D. Ogawa, E. Ikeda, H. Okano, S. Yamanaka, *Nat. Biotechnol.* **2009**, *27*, 743–745.
[5] A. S. Lee, C. Tang, F. Cao, X. Xie, K. van der Bogt, A. Hwang, A. J. Connolly, R. C. Robbins, J. C. Wu, *Cell Cycle* **2009**, *8*, 2608–2612.
[6] O. Naujok, J. Kaldrack, T. Taivankhuu, A. Jorns, S. Lenzen, *Stem Cell Rev.* **2010**, *6*, 450–461.
[7] S. Chung, B. S. Shin, E. Hedlund, J. Pruszak, A. Ferree, U. J. Kang, O. Isacson, K. S. Kim, *J. Neurochem.* **2006**, *97*, 1467–1480.
[8] D. Scadden, A. Srivastava, *Cell Stem Cell* **2012**, *10*, 149–150.
[9] C. Tang, A. S. Lee, J. P. Volkmer, D. Sahoo, D. Nag, A. R. Mosley, M. A. Inlay, R. Ardehali, S. L. Chavez, R. R. Pera, B. Behr, J. C. Wu, I. L. Weissan, M. Drukker, *Nat. Biotechnol.* **2011**, *29*, 829–834.
[10] A. B. Choo, H. L. Tan, S. N. Ang, W. J. Fong, A. Chin, J. Lo, L. Zheng, H. Hentze, R. J. Philp, S. K. Oh, M. Yap, *Stem Cells* **2008**, *26*, 1454–1463.

[11] U. Ben-David, Q. F. Gan, T. Golan-Lev, P. Arora, O. Yanuka, Y. S. Oren, A. Leikin Frenkel, M. Graf, R. Garippa, M. Boehringer, G. Gromo, N. Benvenisty, *Cell Stem Cell* **2013**, *12*, 167 – 179.
[12] M. Richards, C. W. Phoon, G. T. W. Goh, E. K. Seng, X. M. Guo, C. M. F. Tan, W. K. Chan, J. M. K. Lee, *PLOS ONE* **2014**, *9*, e85039.
[13] M. O. Lee, S. H. Moon, H. C. Jeong, J. Y. Yi, T. H. Lee, S. H. Shim, Y. H. Rhee, S. H. Lee, S. J. Oh, M. Y. Lee, M. J. Han, Y. S. Cho, H. M. Chung, K. S. Kim, H. J. Cha, *P. Natl. Acad. Sci. USA* **2013**, *110*, E3281 – 3290.
[14] B. Blum, O. Bar-Nur, T. Govan-Lev, N. Benvenisty, *Nature Biotech.* **2009**, *27*, 281 – 287.
[15] T. Nakahara, M. Takeuchi, I. Kinoyama, T. Minematsu, K. Shirasuna, A. Matsuhisa, A. Kita, F. Tominaga, K. Yamanaka, M. Kudoh, M. Sasamata, *Cancer Res.* **2007**, *67*, 8014 – 8021.
[16] T. Nakahara, A. Kita, K. Yamanaka, M. Mori, N. Amino, M. Takeuchi, F. Tominaga, I. Kinoyama, A. Matsuhisa, M. Kudoh, M. Sasamata, *Cancer Sci.* **2011**, *102*, 614 – 621.
[17] S. H. S. Ho, M. Y. Sim, W. L. S. Yee, T. M. Yang, S. P. J. Yuen, M. L. Go, *Eur. J. Med.Chem.* **2015**, *104*, 42 – 56.
[18] A. Rauch, D. Hennig, C. Schäfer, M. Wirth, C. Marx, T. Heinzel, G. Schneider, O. H. Krämer, *Biochim. Biophys. Acta Rev. Cancer* **2014**, *1845*, 202 – 220.
[19] S. A. Przyborski, V. B. Christie, M. W. Hayman, R. Stewart, G. M. Horrocks, *Stem Cells Dev.* **2004**, *13*, 400 – 408.
[20] R. Pal, G. Ravindran, *Cell Prolif.* **2006**, *39*, 585 – 598.
[21] K. Takahashi, K. Tanabe, M. Ohnuki, M. Narita, T. Ichisaka, K. Tomoda, S. Yamanaka, *Cell* **2007**, *131*, 861 – 872.
[22] K. Takahashi, S. Yamanaka, *Cell* **2006**, *126*, 663 – 676.
[23] J. Yu, M. A. Vodyanik, K. Smuga-Otto, J. Antoslewicz-Bourget, J. L. Frane, S. Tian, J. Nie, G. A. Jonsdottir, V. Routti, R. Stewart, I. I. Slukvin, J. A. Thompson, *Sci.* **2007**, *318*, 1917 – 1920.
[24] M. Asahi, S. Ito, Y. Ishida, *Clin. Lymphoma Myeloma Leuk.* **2015**, *15*, e237.
[25] V. Wagner, D. Hose, A. Seckinger, L. Weiz, T. Meißner, T. Reme, I. Breitkreutz, K. Podar, A. D. Ho, H. Goldschmidt, A. Kramer, B. Klein, M. S. Raab, *Oncotarget* **2014**, *5*, 10237 – 10250.
[26] K. M. Loh, B. Lim, *Cell Stem Cell* **2011**, *8*, 363 – 369.
[27] R. Jaenisch, R. Young, *Cell* **2008**, *132*, 567 – 582.
[28] K. Takahashi, S. Yamanaka, *Nat. Rev. Mol. Cell. Biol.* **2016**, *17*, 183 – 193.
[29] S. Zhang, W. Cui, *World J. Stem Cells* **2014**, *6*, 305 – 311.
[30] Z. Wang, E. Oron, B. Nelson, S. Razis, N. Ivanova, *Cell Stem Cell* **2012**, *10*, 440 – 454.
[31] S. H. Ho, A. Ali, T. M. Chin, M. L. Go, *Oncotarget* **2016**, *7*, 11625 – 11636.
[32] O. Takase, M. Yoshikawa, M. Idei, J. Hirahashi, T. Fujita, T. Takato, T. Isagawa, G. Nagae, H. Suemori, H. Aburatani, K. Hishikawa, *PLOS ONE* **2013**, *8*, e56399.
[33] L. Armstrong, O. Hughes, S. Yung, L. Hyslop, R. Stewart, I. Wappler, H. Peters, T. Walter, P. Stojkovic, J. Evans, M. Stojkovic, M. Lako, *Hum. Mol. Genet.* **2006**, *15*, 1894 – 1913.
[34] D. C. Altieri, *Cancer Lett.* **2013**, *332*, 225 – 228.

Received: May 22, 2016
Revised: June 27, 2016
Published online on ■■ ■■, 0000

Removing the rogues: The safety of stem cell therapy depends on the removal of undifferentiated rogue cells, which would otherwise transform into a malignant phenotype. The potent and selective stemotoxic properties of dioxonaphthoimidazoliums highlight their potential as stem cell clearing agents that could be deployed for this purpose.

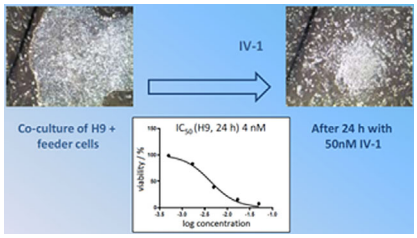

*S.-H. S. Ho, A. Ali, Y.-C. Ng, K.-K. M. Lam, S. Wang, W.-K. Chan, T.-M. Chin, M.-L. Go**

■■ – ■■

Dioxonaphthoimidazoliums are Potent and Selective Rogue Stem Cell Clearing Agents with SOX2-Suppressing Properties